

# Bimetallic $\eta^6, \eta^1$ NCN-Pincer Ruthenium Palladium Complexes with $\eta^6$ -RuCp Coordination: Synthesis, X-ray Structures, and Catalytic Properties<sup>†</sup>

Sylvestre Bonnet,<sup>†</sup> Joop H. van Lenthe,<sup>‡</sup> Maxime A. Siegler,<sup>§</sup> Anthony L. Spek,<sup>§</sup>  
Gerard van Koten,<sup>†</sup> and Robertus J. M. Klein Gebbink<sup>\*,†</sup>

*Chemical Biology & Organic Chemistry, Debye Institute for Nanomaterials Science, Faculty of Science, Utrecht University, Padualaan 8, 3584 CH Utrecht, The Netherlands, Theoretical Chemistry Group, Debye Institute for Nanomaterials Science, Faculty of Science, Utrecht University, Padualaan 8, 3584 CH Utrecht, The Netherlands, and Crystal and Structural Chemistry, Bijvoet Center for Biomolecular Research, Faculty of Science, Utrecht University, Padualaan 8, 3584 CH Utrecht, The Netherlands*

Received December 19, 2008

The synthesis, structure, and catalytic activity of a series of bimetallic  $\eta^6, \eta^1$ -NCN-pincer ruthenium palladium complexes,  $[3]^+$ – $[5]^+$ , have been studied, in which  $\eta^6$ -coordination of  $[\text{Ru}(\text{C}_5\text{R}_5)]^+$  (R = H or Me) is realized either directly to the central arene ring of the NCN-pincer palladium complex ( $[3]^+$  and  $[4]^+$ ) or to the *para*-phenyl substituent ( $[5]^+$ ). The X-ray structures of  $[4]^+$  and  $[5]^+$ , as well as the regioselectivity observed in the synthesis of  $[5]^+$ , provide clear evidence of intramolecular steric interactions in  $[4]^+$  between the amine arms of the pincer moiety and the methyl groups of the cyclopentadienyl ligand. Cyclovoltammetry data point to strong electronic interactions between the two metal fragments in  $[3]^+$  and  $[4]^+$  and only limited interactions in  $[5]^+$ . Catalytic studies in the cross-coupling reaction between *trans*-phenylvinylboronic acid and vinyl epoxide show that the catalytic activity of the palladium center is enhanced by  $\eta^6$ -coordination of the ruthenium fragment. These modifications of the catalytic activity of palladium are not correlated to the decreased electron density on palladium, as confirmed by DFT calculations. We hence propose a mechanism in which transmetalation is the rate-determining step.

## Introduction

Palladium complexes have been extensively used as catalysts in a wide range of carbon–carbon bond-forming reactions,<sup>1,2</sup> not only in homogeneous media,<sup>3,4</sup> but also on a solid support.<sup>5–10</sup> Among the many different ligands that have been studied for these reactions in combination with Pd, the NCN-

pincer ligand offers some special features.<sup>3,11–13</sup> First, the terdentate framework of the NCN-pincer ligand stabilizes the carbon-to-palladium bond. In addition, by occupying three out of the four coordination sites on the metal center, the number of catalytic intermediates is restricted, which can improve selectivity.<sup>14</sup> These peculiar properties of the NCN-pincer framework have opened the door to new, selective organic reactions of allyl halides,<sup>15</sup> stannanes,<sup>16</sup> and boronic acids.<sup>17–19</sup>

Up to now, two different approaches have been developed to tune the catalytic activity and selectivity of NCN-pincer palladium complexes: (1) substitution by electron-donating or electron-withdrawing groups in *para*-position to the carbon-to-palladium bond, which modifies the electron density on palladium,<sup>13,20,21</sup> and (2) changing the size and geometry of the organic substituents borne by the nitrogen atoms, notably to induce stereoselectivity.<sup>22–25</sup>

<sup>†</sup> Dedicated to the late Professor Yoshihiko Ito (deceased Dec 23rd, 2006), in commemoration of a long friendship and fine collaboration. We would like to honor his outstanding contribution in the fields of synthetic chemistry and organometallic chemistry.

\* Corresponding author. E-mail: r.j.m.kleingebink@uu.nl. Fax: +31 30 2523615.

<sup>†</sup> Chemical Biology & Organic Chemistry, Debye Institute for Nanomaterials Science.

<sup>§</sup> Theoretical Chemistry Group, Debye Institute for Nanomaterials Science.

<sup>§</sup> Bijvoet Center for Biomolecular Research.

(1) Tsuji, J. *Palladium Reagents and Catalysts: New Perspectives for the 21st Century*; Wiley: Weinheim, Germany, 2004.

(2) Tsuji, J. *Palladium in Organic Synthesis*; Springer: Berlin, Germany, 2005.

(3) Singleton, J. T. *Tetrahedron* **2003**, *59*, 1837.

(4) Albrecht, M.; van Koten, G. *Angew. Chem., Int. Ed.* **2001**, *40*, 3750.

(5) Song, C. E.; Lee, S. G. *Chem. Rev.* **2002**, *102*, 3495.

(6) Leadbeater, N. E.; Marco, M. *Chem. Rev.* **2002**, *102*, 3217.

(7) Choplin, A.; Quignard, F. *Coord. Chem. Rev.* **1998**, *178–180*, 1679.

(8) Brunel, D.; Bellocq, N.; Sutra, P.; Cauvel, A.; Lasperas, M.; Moreau, P.; Di Renzo, F.; Galarneau, A.; Fajula, F. *Coord. Chem. Rev.* **1998**, *180*, 1085.

(9) Mehendale, N. C.; Sietsma, J. R. A.; de Jong, K. P.; van Walree, C. A.; Klein Gebbink, R. J. M.; van Koten, G. *Adv. Synth. Catal.* **2007**, *349*, 2619.

(10) Mehendale, N. C.; Bezemer, C.; van Walree, C. A.; Klein Gebbink, R. J. M.; van Koten, G. *J. Mol. Catal. A: Chem.* **2006**, *257*, 167.

(11) Morales-Morales, D. *The Chemistry of Pincer Compounds*; Elsevier B. V.: Amsterdam, The Netherlands, 2007.

(12) Szabó, K. *Synlett* **2006**, *6*, 811.

(13) Slagt, M. Q.; Rodriguez, G.; Grutters, M. M. P.; Klein Gebbink, R. J. M.; Klopper, W.; Jenneskens, L. W.; Lutz, M.; Spek, A. L.; van Koten, G. *Chem.–Eur. J.* **2004**, *10*, 1331.

(14) Solin, N.; Kjellgren, J.; Szabó, K. J. *Angew. Chem., Int. Ed.* **2003**, *42*, 3656.

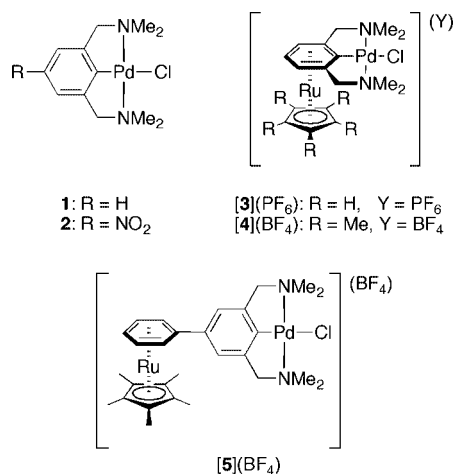
(15) Solin, N.; Kjellgren, J.; Szabó, K. J. *J. Am. Chem. Soc.* **2004**, *126*, 7026.

(16) Wallner, O. A.; Szabó, K. J. *Org. Lett.* **2004**, *6*, 1829.

(17) Olsson, V. J.; Sebelius, S.; Selander, N.; Szabó, K. J. *J. Am. Chem. Soc.* **2006**, *128*, 4588.

(18) Solin, N.; Wallner, O. A.; Szabó, K. J. *Org. Lett.* **2005**, *7*, 698.

(19) Kjellgren, J.; Aydin, J.; Wallner, O. A.; Saltanova, I. V.; Szabó, K. J. *Chem.–Eur. J.* **2005**, *11*, 5260.

**Scheme 1. NCN-Pincer Palladium and Bimetallic Palladium Ruthenium Complexes Used in This Study**


Recently,<sup>26</sup> we explored a third approach for influencing the reactivity of the metal center of NCN-pincer metal compounds. We showed that  $\eta^6$ -coordination of the organometallic fragment [Ru(C<sub>5</sub>R<sub>5</sub>)]<sup>+</sup> (R = H or Me) to the central arene ring of a platinated or, notably, a palladated NCN-pincer ligand can be realized in a direct electrophilic reaction affording heterobimetallic products, e.g., [3]<sup>+</sup> and [4]<sup>+</sup> in Scheme 1, in high yield. In these  $\eta^6, \eta^1$ -heterobimetallic architectures the  $\sigma$ - and  $\pi$ -electrons of one unique phenyl anion arrange the metal-to-carbon interactions in an orthogonal fashion. As shown in our initial communication, the redistribution of electrons in these systems is large, which results in an electron-poor NCN-pincer metal center. However, the difference in charge between monometallic complex 1 and cationic complexes of type [3]<sup>+</sup> and [4]<sup>+</sup> hampers a direct comparison of their electrochemical and/or chemical properties.

For that reason,  $\eta^6, \eta^1$ -NCN-pincer bimetallic complexes of type [5]<sup>+</sup> (Scheme 1) were considered, in which  $\eta^6$ -coordination occurs at the *para*-phenyl substituent, and not at the arene ring of the pincer moiety. In this paper, we describe the synthesis of complex [5]<sup>+</sup>, as well as the application of the palladium-containing complexes [3]<sup>+</sup>–[5]<sup>+</sup> in the catalytic cross-coupling reaction between *trans*-phenylvinylboronic acid and vinyl epoxide.<sup>19</sup> It appeared that  $\eta^6$ -coordination made the resulting pincer ruthenium palladium compounds faster catalysts. Electrochemical measurements and DFT calculations were carried out to substantiate the electron richness of palladium and link the catalytic performance of these unique mixed Ru–Pd compounds to the most plausible mechanism.

(20) Dijkstra, H. P.; Slagt, M. Q.; McDonald, A.; Kruihof, C. A.; Kreiter, R.; Mills, A. M.; Lutz, M.; Spek, A. L.; Klopper, W.; van Klink, G. P. M.; van Koten, G. *Eur. J. Inorg. Chem.* **2003**, 830.

(21) Koecher, S.; Walfort, B.; Mills, A. M.; Spek, A. L.; van Klink, G. P. M.; van Koten, G.; Lang, H. *J. Organomet. Chem.* **2008**, 693, 1991.

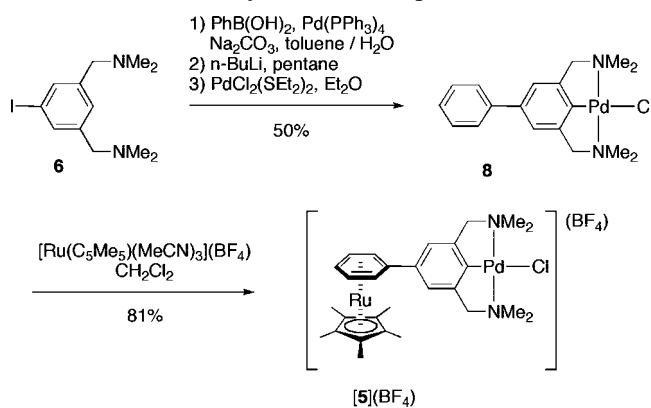
(22) Gosiewska, S.; Herreras, S. M.; Lutz, M.; Spek, A. L.; Havenith, R. W. A.; van Klink, G. P. M.; van Koten, G.; Klein Gebbink, R. J. M. *Organometallics* **2008**, 27, 2549.

(23) Gosiewska, S.; Martinez, S. H.; Lutz, M.; Spek, A. L.; van Koten, G.; Klein Gebbink, R. J. M. *Eur. J. Inorg. Chem.* **2006**, 4600.

(24) Gosiewska, S.; Veld, M. F. I.; de Pater, J. J. M.; Bruijninx, P. C. A.; Lutz, M.; Spek, A. L.; van Koten, G.; Klein Gebbink, R. J. M. *Tetrahedron: Asymmetry* **2006**, 17, 674.

(25) Takenaka, K.; Minakawa, M.; Uozumi, Y. *J. Am. Chem. Soc.* **2005**, 127, 12273.

(26) Bonnet, S.; Lutz, M.; Spek, A. L.; van Koten, G.; Klein Gebbink, R. J. M. *Organometallics* **2008**, 27, 159.

**Scheme 2. Synthesis of Complex [5](BF<sub>4</sub>)**

**Results**

**Synthesis and X-ray Structure of [5](BF<sub>4</sub>).** The synthetic route toward complex [5](BF<sub>4</sub>) is shown in Scheme 2. The Ph-NCN-pincer arene ligand 7 was synthesized by a Suzuki cross-coupling reaction of I-NCN-pincer ligand 6 with phenylboronic acid.<sup>27</sup> Then, lithiation of 7 at  $-78$  °C in pentane with n-BuLi, followed by reaction with PdCl<sub>2</sub>(SEt<sub>2</sub>)<sub>2</sub> in diethyl ether, afforded the *para*-phenyl-substituted NCN-pincer palladium complex 8.<sup>20</sup> Subsequent reaction of 8 with [Ru(C<sub>5</sub>Me<sub>5</sub>)]<sup>+</sup> using [Ru(C<sub>5</sub>Me<sub>5</sub>)(MeCN)<sub>3</sub>](BF<sub>4</sub>) in dichloromethane at room temperature afforded [5](BF<sub>4</sub>) in 50% yield (based on 7). <sup>1</sup>H NMR spectra of the product clearly showed that the reaction is regioselective:  $\eta^6$ -coordination at the  $\eta^1$ -palladated arene ring had not taken place (see Scheme 2), but instead selective  $\eta^6$ -coordination to the *para*-phenyl group had occurred. For complex [5]<sup>+</sup> indeed, the protons of the  $\eta^6$ -coordinated arene ring appear at low field (three signals between 6.1 and 6.6 ppm in acetone-*d*<sub>6</sub>), whereas the singlet of the *meta* protons on the  $\eta^1$ -coordinated ring remains around 7.3 ppm (in acetone-*d*<sub>6</sub>).<sup>28</sup> Unlike in [3]<sup>+</sup> and [4]<sup>+</sup>, where facial differentiation of the pincer moiety induced by the ruthenium fragment leads to two different (diastereotopic) methyl groups and two different (diastereotopic) methylene protons,<sup>26</sup> in [5]<sup>+</sup> there is only one methyl group and one methylene proton for the NCN-pincer arms, which shows that rotation around the single, central C4–C1' bond of the  $\eta^6, \eta^1$ -coordinated biphenyl ligand is fast at room temperature, i.e., there is no facial differentiation of the pincer moiety induced by the  $\eta^6$ -coordinated ruthenium fragment in [5]<sup>+</sup>. Much like [3](PF<sub>6</sub>) and [4](BF<sub>4</sub>), complex [5](BF<sub>4</sub>) has good solubilities in organic solvents such as acetone and dichloromethane, and gives a white solid upon precipitation from pentane.

Colorless crystals of [5](BF<sub>4</sub>) suitable for X-ray analysis were obtained by slow vapor diffusion of hexane into a dichloromethane solution of [5](BF<sub>4</sub>) (see Experimental Part). In the solid state, [5](BF<sub>4</sub>) was found to be isomorphous to its platinum analogue.<sup>29</sup>

There are two crystallographically independent molecules in the asymmetric unit and, after least-squares refinements, the atomic displacement ellipsoids of the two independent molecular cations were satisfactory (see Figure 1). Table 1 includes selected distances and angles for the molecular structure of

(27) Rodriguez, G.; Albrecht, M.; Schoenmaker, J.; Ford, A.; Lutz, M.; Spek, A. L.; van Koten, G. *J. Am. Chem. Soc.* **2002**, 124, 5127.

(28) In Ph-NCNPdCl (8), all aromatic protons appear at lower fields, i.e., between 7.0 and 8.0 ppm (in CD<sub>2</sub>Cl<sub>2</sub>).

(29) Bonnet, S.; van Lenthe, J. H.; Siegler, M. A.; Lutz, M.; Spek, A. L.; van Koten, G.; Klein Gebbink, R. J. M., submitted.

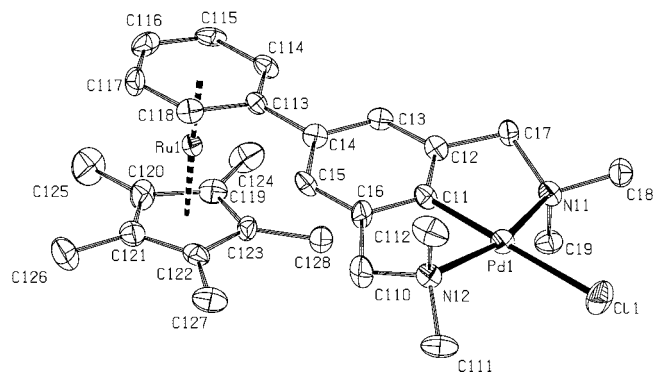


**Figure 1.** Displacement ellipsoid plot (drawn at 50% probability level) of one of the two crystallographically independent cations in the asymmetric unit of  $[5](\text{BF}_4)$  at 150 K.  $\text{BF}_4^-$  counteranions and H-atoms have been omitted for clarity.

cation  $[5]^+$ , as well as those for the neutral complex **2**,<sup>30</sup> the related bimetallic cationic complex  $[4]^+$ ,<sup>26</sup> and the ruthenium complex  $[\text{Ru}(\text{C}_5\text{Me}_5)(\eta^6\text{-}1,3\text{-}(\text{Me}_2\text{NCH}_2)_2\text{C}_6\text{H}_4)](\text{BF}_4)$ , denoted  $[9]^+$ .<sup>31</sup>

The molecular structure of  $[5]^+$  clearly shows that the palladium center is  $\eta^1$ -coordinated to  $\text{C}_{ipso}$  of the NCN-pincer ligand, whereas the ruthenium center is  $\eta^6$ -coordinated to the *para*-phenyl substituent. Unlike in  $[4]^+$ , there is no indication for steric constraints in  $[5]^+$  between the  $\text{C}_5\text{Me}_5$  ligand and the N-methyl groups. The Ru–C distances are very similar, and the planes defined by the  $\eta^6$ -arene ring and the  $\text{Cp}^*$  ligand are nearly parallel. The approximate  $\text{C}_2$  symmetry of the pincer fragment observed for this family of compounds is also present in  $[5]^+$ .

**Electrochemical Properties.** In order to get information about the electron density on the Pd center in the Pd–Ru complexes, cyclic voltammograms of the neutral palladium (**1**, **2**, **8**) and cationic palladium–ruthenium ( $[3]^+$ ,  $[4]^+$ , and  $[5]^+$ ) complexes were recorded in acetonitrile (see Table 2). For all NCN-pincer palladium complexes, an irreversible oxidation wave was observed, which corresponds to the  $\text{Pd}^{\text{II}}/\text{Pd}^{\text{IV}}$  oxidation.<sup>32</sup> For **2**, an additional reversible reduction wave was observed at  $E_{1/2} = -1.64$  V vs  $\text{Fc}/\text{Fc}^+$ , which corresponds to the formation of the *para*- $\text{NO}_2^-$  radical anion.<sup>33</sup> Reduction of the ruthenium center in  $[\text{Ru}(\eta^6\text{-arene})(\eta^5\text{-C}_5\text{R}_5)]^+$  complexes is known to occur at very low potentials<sup>34</sup> and could not be observed for the bimetallic cations  $[3]^+ - [5]^+$ . Overall, our results show that  $\eta^6$ -coordination of the ruthenium fragment directly to the arene ring of the pincer framework as in  $[3]^+$  and  $[4]^+$  induces a very large shift of the  $\text{Pd}^{\text{II}}/\text{Pd}^{\text{IV}}$  oxidation potential ( $\Delta E_{\text{ox}} = +240$  mV compared to complex **1**). This shift is even larger than that induced by a *para*- $\text{NO}_2$  substituent ( $\Delta E_{\text{ox}} = +120$  mV) in the parent pincer palladium complex **2**. When  $\eta^6$ -coordination takes place to a *para*-phenyl substituent as in  $[5]^+$ , the shift of the oxidation potential is much weaker ( $\Delta E_{\text{ox}} = 20$  mV compared to **8**).

**Catalytic Properties.** The catalytic performances of  $[3]^+$ ,  $[4]^+$ , and  $[5]^+$  in the cross-coupling reaction of *trans*-phenylvinylboronic acid and vinyl epoxide were tested (see Scheme 3)<sup>19</sup> and compared with those of the neutral complexes **1**, **2**, and **8** (see Table 3 and Figure 2). All NCN-pincer palladium complexes are active homogeneous catalysts and lead to good yields at full conversion. In order to monitor the reaction in time, the catalyst loading was lowered to 1 and 0.25 mol %, respectively (cf. the use of 2.5 mol % in the original publication),<sup>19</sup> while the amount of water was substantially increased (+25%). Figures 2 and 3 depict the reaction profiles analyzed by gas chromatography, i.e., the total yields of the reaction products (linear + branched) versus time and nature of the catalyst, and the linear/branched ratio versus time and nature of the catalyst, respectively. When 1 mol % catalyst was used, the best catalysts (**2** and  $[5]^+$ ) are able to lead the reaction to completion within 2 h (which regrettably was too fast to obtain satisfactory kinetic data using the available ChemSpeed apparatus); with 0.25 mol % catalyst the reaction required 6–24 h to go to completion, leading to satisfactory kinetic data (Figure 2). In all cases, an initial induction period was observed, which resulted for the most active catalysts in a time profile that has a sigmoidal shape. Table 3 gives GC yields after 2 h using 1 mol % catalyst and the time ( $t_{50}$ ) necessary to reach 50% conversion using 0.25 mol % catalyst. Interestingly, for all catalysts the linear/branched ratio gradually increased during the course of the reaction until it had reached the value observed for  $[\text{PdBr}(\text{H-NCN})]$  ( $l/b = 2.33$ , see Figure 3).<sup>19</sup>

**DFT Calculations.** In order to investigate whether the observed trends in catalysis can be explained in terms of electronic effects, we performed DFT calculations based on the B3LYP/LANL2DZ method as implemented in the GAMESS-UK program.<sup>35</sup> In a recent publication, the mechanism proposed for the SeCSe-pincer palladium-catalyzed reaction comprised two steps: (i) transmetalation between the boronic acid and the palladium complex, yielding a *trans*-phenylvinyl SeCSe-pincer palladium intermediate, and (ii) the nucleophilic attack of this transmetalated intermediate to vinyl epoxide in an  $\text{S}_{\text{N}}2$ -type mechanism.<sup>19</sup>

We minimized by DFT the five intermediates  $[\text{IS}_n]$  ( $n = 1-5$ ) obtained by transmetalation of *trans*-phenylvinylboronic acid with the NCN-pincer palladium catalysts **1**, **2**,  $[3]^+$ ,  $[4]^+$ , and  $[5]^+$ , respectively (see Scheme 4). In  $[\text{IS}_n]$ , the chloride anion coordinated to palladium has been replaced by a *trans*-phenylvinyl organic ligand. In order to be able to compare charged and neutral species, all cationic complexes were minimized in the presence of an additional chloride counteranion. In all five minimized geometries, the plane of the  $\text{PhC}_2\text{H}_2$  ligand coordinated in a  $\eta^1$ -fashion to Pd was found perpendicular to the plane of the arene ring, making an angle of  $\sim 80^\circ$  with the coordination plane of Pd (see Figure 4). Table 4 gives for  $[\text{IS}_n]$  ( $n = 1-5$ ) the natural charges ( $Q$ ) on Pd,  $\text{C}_{ipso}$ , and  $\text{C}_{\text{vinyl}}$ ,<sup>36</sup> the bond index (BI)<sup>38</sup> of the Pd– $\text{C}_{\text{vinyl}}$  bond, and the energy level  $E_\sigma$  of the highest filled molecular orbital of  $\sigma$  character

(30) Slagt, M. Q.; Dijkstra, H. P.; McDonald, A.; Klein Gebbink, R. J. M.; Lutz, M.; Ellis, D. D.; Mills, A. M.; Spek, A. L.; van Koten, G. *Organometallics* **2003**, *22*, 27.

(31) Siegler, M. A.; Bonnet, S.; Schreurs, A. M. M.; Klein Gebbink, R. J. M.; van Koten, G.; Spek, A. L., submitted.

(32) Gagliardo, M.; Rodriguez, G.; Dam, H. H.; Lutz, M.; Spek, A. L.; Havenith, R. W. A.; Coppo, P.; De Cola, L.; Hartl, F.; van Klink, G. P. M.; van Koten, G. *Inorg. Chem.* **2006**, *45*, 2143.

(33) Chauhan, B. G.; Fawcett, W. R.; Lasia, A. J. *Phys. Chem.* **1977**, *81*, 1476.

(34) Gusev, O. V.; Ievlev, M. A.; Peterleitner, M. G.; Peregodova, S. M.; Denisovich, L. I.; Petrovskii, P. V.; Ustyynyuk, N. A. *Russ. Chem. Bull.* **1996**, *45*, 1601.

(35) Guest, M. F.; Bush, I. J.; van Dam, H. J. J.; Sherwood, P.; Thomas, J. M. H.; van Lenthe, J. H.; Havenith, R. W. A.; Kendrick, J. *Mol. Phys.* **2005**, *103*, 719.

(36)  $\text{C}_{ipso}$  and  $\text{C}_{\text{vinyl}}$  are the two carbon atoms bound to Pd and belonging to, respectively, the arene ring of the NCN-pincer ligand or the double bond of the *trans*-phenylvinyl ligand, respectively.

(37) Reed, A. E.; Curtiss, L. A.; Weinhold, F. *Chem. Rev.* **1988**, *88*, 899.

(38) Stradella, O. G.; Villar, H. O.; Castro, E. A. *Theor. Chim. Act.* **1986**, *70*, 67.

**Table 1.** Selected Distances and Angles in the Crystal Structures of Monometallic Complexes [Ru(C<sub>5</sub>Me<sub>5</sub>)(η<sup>6</sup>-1,3-(Me<sub>2</sub>NCH<sub>2</sub>)<sub>2</sub>C<sub>6</sub>H<sub>4</sub>)](BF<sub>4</sub>)<sup>+</sup>{[9](BF<sub>4</sub>)} and 2 and Bimetallic Complexes [4](BF<sub>4</sub>)<sup>c</sup> and [5](BF<sub>4</sub>)<sup>d</sup>

distance (Å) and angles (deg)	[9](BF <sub>4</sub> ) <sup>a</sup>	2 <sup>b</sup>	[4](BF <sub>4</sub> ) <sup>c</sup>	[5](BF <sub>4</sub> ) <sup>d</sup>
<i>d</i> (Pd–C <sub>1</sub> )		1.914(2)	1.9122(14)	1.911(8)
<i>d</i> (Pd–Cl)		2.4280(17)	2.4236(4)	2.411(2)
<i>d</i> (Pd–N <sub>1</sub> )		2.102(2)	2.1104(3)	2.115(7)
<i>d</i> (Pd–N <sub>2</sub> )		2.101(2)	2.1097(12)	2.113(7)
θ(N <sub>1</sub> –Pd–N <sub>2</sub> )		163.53(9)	164.05(5)	162.5(3)
θ(Cl–Pd–C <sub>1</sub> )		172.78(9)	175.86(4)	179.7(2)
θ(PdN <sub>1</sub> N <sub>2</sub> C <sub>1</sub> –C <sub>1</sub> C <sub>2</sub> C <sub>6</sub> )		6.8(2)	11.45(6)	12.0(11)
<i>d</i> (Ru–arene)				
- to average plane	1.6997(16)		1.72304(12)	1.7014(7)
- to carbon (shortest)	2.199(7)		2.1869(15)	2.185(8)
- to carbon (longest)	2.222(7)		2.2847(14)	2.226(9)
<i>d</i> (Ru–C <sub>5</sub> Me <sub>5</sub> )	1.8096(6)		1.81396(12)	1.8009(7)
θ(arene–C <sub>5</sub> Me <sub>5</sub> )	1.1(5)		7.35(8)	3.4(5)
<i>d</i> (Ru–Pd)			3.9150(2)	7.6945(9)
biphenyl angle				13.2(13)
				15.2(13)

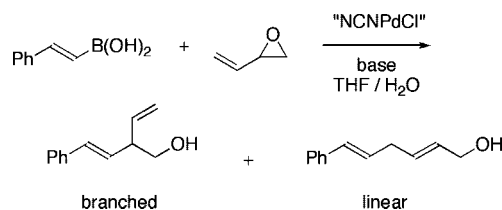
<sup>a</sup> Four very similar but distinct geometries are found in the unit cell of the low-*T* structure of [9]<sup>+</sup> (150 K); only the geometry of one cation (that containing Ru1) is shown here; see ref 31. <sup>b</sup> See ref 30. <sup>c</sup> See ref 26. <sup>d</sup> This work.

**Table 2.** Pd<sup>II</sup>/Pd<sup>IV</sup> Oxidation Potentials As Measured by Cyclic Voltammetry<sup>a</sup>

complex	<i>E</i> <sub>ox</sub> (Pd <sup>II</sup> /Pd <sup>IV</sup> ), V
1	+0.68
2 <sup>b</sup>	+0.80
[3] <sup>+</sup>	+0.92
[4] <sup>+</sup>	+0.93
[5] <sup>+</sup>	+0.68
8	+0.66

<sup>a</sup> Conditions: Pt electrode, scan rate 100 mV s<sup>-1</sup>, 0.1 M Bu<sub>4</sub>NPF<sub>6</sub> in acetonitrile, Fc/Fc<sup>+</sup> as internal reference. All Pd<sup>II</sup>/Pd<sup>IV</sup> oxidations are electrochemically irreversible. <sup>b</sup> In addition to the irreversible Pd<sup>II</sup>/Pd<sup>IV</sup> oxidation, the reversible one-electron reduction of the *para*-NO<sub>2</sub> group is observed at *E*<sub>1/2</sub> = -1.64 V (see text).

### Scheme 3. Cross-Coupling Reaction between *trans*-Phenylvinylboronic Acid and Vinyl Epoxide Catalyzed by NCN-Pincer Palladium Complexes

**Table 3.** Catalytic Properties of NCN-Palladium Pincer Complexes in the Cross-Coupling Reaction between *trans*-Phenylvinylboronic Acid and Vinyl Epoxide<sup>a</sup>

catalyst	GC yield (%) after 2 h <sup>b</sup>	<i>t</i> <sub>50</sub> (h) <sup>c</sup>
1	29	9.7
2	98	3.3
8	22	7.0
[3](PF <sub>6</sub> )	77	4.5
[4](BF <sub>4</sub> )	63	8.5
[5](BF <sub>4</sub> )	93	3.0

<sup>a</sup> *t*<sub>50</sub> is defined as the time necessary to reach 50% conversion. Conditions: 1.6 mmol of boronic acid, 1.2 eq. of epoxide, 2 equiv of Cs<sub>2</sub>CO<sub>3</sub>, 25 °C, THF/H<sub>2</sub>O 7.5:1. GC yields were determined using di(*n*-hexyl) ether as internal standard. For comparison, under Szabó's conditions (0.16 mmol of epoxide, 1.2 equiv of boronic acid, 2 equiv of Cs<sub>2</sub>CO<sub>3</sub>, 2.5 mol % [PdBr(H-NCN)], 20 °C, THF/H<sub>2</sub>O 10:1) the isolated yield after 4 h is 95% and the lin/br ratio is 2.3.<sup>19</sup> <sup>b</sup> Using 1 mol % catalyst. <sup>c</sup> Using 0.25 mol % catalyst.

corresponding to the Pd–C<sub>vinyl</sub> bond (HOMO–1 for [IS<sub>1</sub>–2], HOMO–5 for [IS<sub>3</sub>–5]).

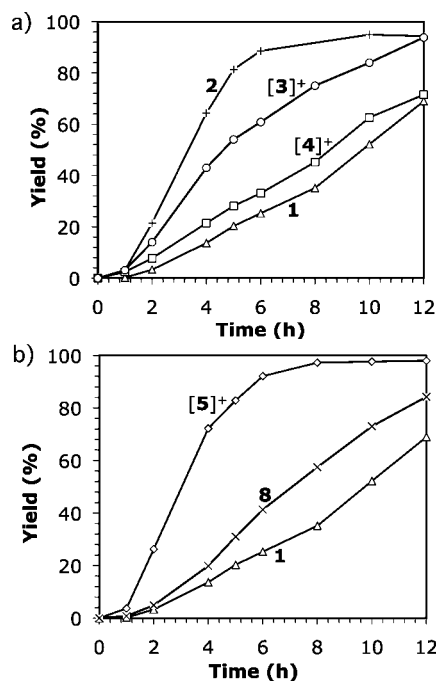


**Figure 2.** Monitoring the cross-coupling reaction between *trans*-phenylvinylboronic acid and vinyl epoxide, depending on the nature of the catalyst. Total yields (linear + branched products) as a function of time. Conditions: 1.6 mmol of boronic acid, 1.2 equiv of epoxide, 2 equiv of Cs<sub>2</sub>CO<sub>3</sub>, 0.25 mol % in Pd catalyst, 2 equiv of Cs<sub>2</sub>CO<sub>3</sub>, 25 °C, THF/H<sub>2</sub>O 7.5:1, di(*n*-hexyl) ether (internal standard).

According to these calculations, when following the series [IS<sub>1</sub>], [IS<sub>5</sub>], [IS<sub>2</sub>], [IS<sub>4</sub>], [IS<sub>3</sub>] the following trends are observed (see Table 4): (1) the positive charge on palladium increases consistently with the evolution of the Pd<sup>II</sup>/Pd<sup>IV</sup> oxidation potentials as measured by cyclic voltammetry (see Table 3); (2) the energy level *E*<sub>σ</sub> and the charge *Q*(C<sub>vinyl</sub>) decrease, which corresponds to a decreasing nucleophilicity of [IS<sub>*n*</sub>].

## Discussion

The synthesis of the bimetallic ruthenium–palladium complexes [3]<sup>+</sup>–[5]<sup>+</sup> demonstrates the generality of the applied organometallic synthetic route. η<sup>6</sup>-Coordination of the [Ru(C<sub>5</sub>Me<sub>5</sub>)]<sup>+</sup> fragment to one of the arene rings of an NCN-

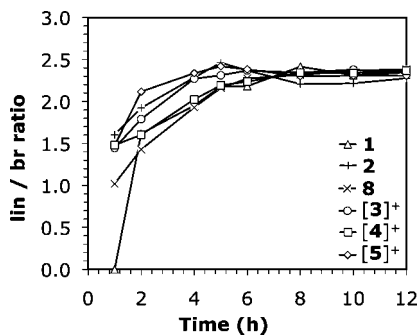
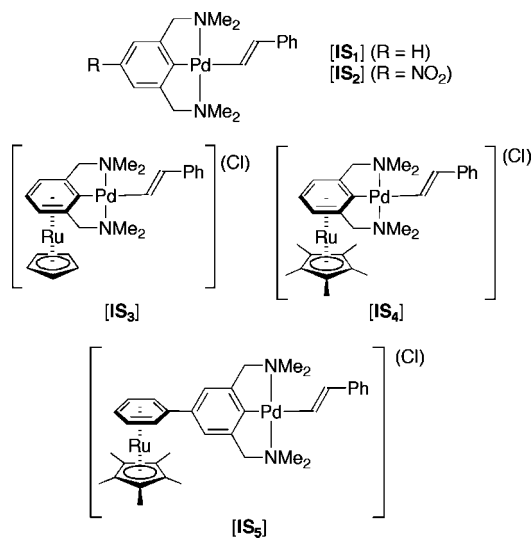


**Figure 3.** Monitoring the cross-coupling reaction between *trans*-phenylvinylboronic acid and vinyl epoxide, depending on the nature of the catalyst (same notations as in Figure 2). Linear/branched ratio as a function of time. Conditions: 1.6 mmol of boronic acid, 1.2 equiv of epoxide, 2 equiv of  $\text{Cs}_2\text{CO}_3$ , 0.25 mol % in Pd catalyst, 2 equiv of  $\text{Cs}_2\text{CO}_3$ , 25 °C, THF/ $\text{H}_2\text{O}$  7.5:1, di(*n*-hexyl) ether (internal standard).

**Scheme 4. Intermediate Species  $[\text{IS}_n]$  ( $n = 1-5$ ) Derived from Catalysts **1**, **2**, **[3]<sup>+</sup>**, **[4]<sup>+</sup>**, and **[5]<sup>+</sup>**, Respectively, by Substitution of a Chloride Ligand by a *trans*-Phenylvinyl Organic Group<sup>a</sup>**



<sup>a</sup> The chloride counteranion has been added to ensure neutral species.

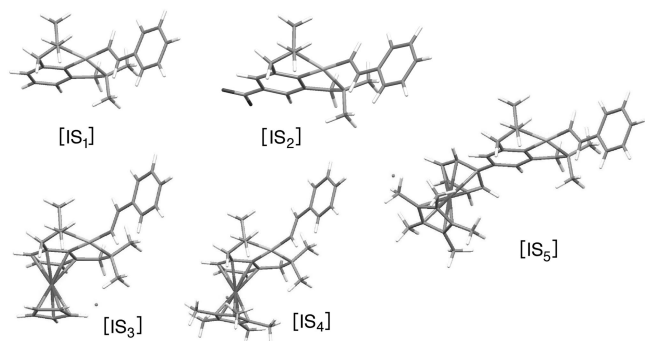


**Figure 4.** DFT-minimized structures of intermediates  $[\text{IS}_n]$  ( $n = 1-5$ ).

pincer palladium complex was realized by a direct reaction of  $[\text{Ru}(\text{C}_5\text{Me}_5)(\text{MeCN})_3]^+$  with the organopalladium complex **1** or **8**; that is, under the chosen reaction conditions  $\eta^6$ -coordination takes place without affecting the carbon-to-palladium bond. The reaction of  $[\text{Ru}(\text{C}_5\text{Me}_5)(\text{MeCN})_3]^+$  with **8** occurs regioselectively at the *para*-phenyl ring. This selectivity most likely results from

**Table 4. Electronic Parameters Calculated by DFT for Palladium-Transmetalated Intermediates  $[\text{IS}_n]$  ( $n = 1-5$ )<sup>a</sup>**

	$\text{IS}_1$	$\text{IS}_5$	$\text{IS}_2$	$\text{IS}_4$	$\text{IS}_3$
$Q(\text{Pd})$	0.610	0.618	0.624	0.629	0.642
$Q(\text{C}_{\text{vinyl}})$	-0.549	-0.547	-0.549	-0.539	-0.533
$Q(\text{C}_{\text{ipso}})$	-0.253	-0.244	-0.224	-0.265	-0.262
$\text{BI}(\text{Pd}-\text{C}_{\text{vinyl}})$	0.774	0.789	0.793	0.808	0.816
$E_\sigma$ (eV) <sup>b</sup>	-5.23	-5.69	-5.76	-5.95	-5.90

<sup>a</sup> The table is ordered according to increasing  $Q(\text{Pd})$  values. <sup>b</sup> Energy of the highest filled molecular orbital of  $\sigma$  character corresponding to the  $\text{Pd}-\text{C}_{\text{vinyl}}$  bond (HOMO-1 for  $[\text{IS}_{1-2}]$ , HOMO-5 for  $[\text{IS}_{3-5}]$ ).

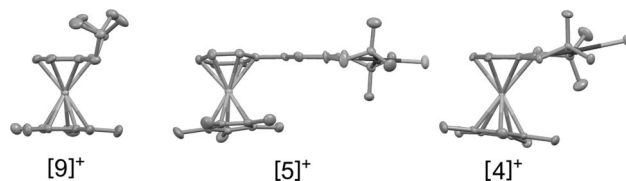


**Figure 5.** Side view of the X-ray structures of complexes **[9]<sup>+</sup>**( $\text{BF}_4$ ), **[5]<sup>+</sup>**( $\text{BF}_4$ ), and **[4]<sup>+</sup>**( $\text{BF}_4$ ).  $\text{BF}_4^-$  counteranions and H-atoms have been omitted for clarity.

steric constraints between the N-methyl groups of the NCN-pincer fragment and the Me groups of the  $\text{Cp}^*$  ligand borne by ruthenium.<sup>29</sup> However, this steric hindrance is small enough not to destabilize  $\eta^6$ -coordination directly to the arene ring of the NCN-pincer metal complex itself as in **[4]<sup>+</sup>**, in which an alternate binding site is absent.<sup>26</sup> For the reaction of the less hindered  $[\text{RuCp}]^+$  fragment with **8** such regioselectivity is not observed, and the reaction yields a mixture of isomers that appeared difficult to separate.

The effect of steric constraints in **[4]<sup>+</sup>** is also apparent by comparing the X-ray structures of **[4]<sup>+</sup>**, **[5]<sup>+</sup>**, and **[9]<sup>+</sup>** (see Figure 5). In compound **[9]<sup>+</sup>** there is no palladium coordinated to the NCN-pincer ligand, and both free amine ligands are located at the opposite side of the arene ring, compared to the ruthenium fragment. In **[5]<sup>+</sup>**, the NCN-pincer palladium pincer fragment induces a weak steric bulk with the  $\text{Cp}^*$  ligand, but the N-methyl groups are still far away from the  $\text{Cp}^*$  methyl groups (cf. the long Pd-Ru distance). In both compounds **[5]<sup>+</sup>** and **[9]<sup>+</sup>** the dihedral angle between the plane of the arene ring and that of the cyclopentadienyl ring is small, and the distance between the ruthenium center and the average plane of the arene ring is short (see Table 1). In **[4]<sup>+</sup>** the ruthenium fragment is directly coordinated to the arene ring of the NCN-pincer palladium moiety, which minimizes the distance between the N-methyl and  $\text{Cp}^*$  methyl groups, hence maximizing steric congestion. Consequently, the arene and cyclopentadienyl ring are no longer parallel, and the Ru-arene distance is elongated (1.72304(12) Å in **[4]<sup>+</sup>** vs 1.7014(7) and 1.7057(8) Å in **[5]<sup>+</sup>**).

The present catalytic studies show that bimetallic ruthenium NCN-pincer complexes **[3]<sup>+</sup>**-**[5]<sup>+</sup>** catalyze the cross-coupling reaction between *trans*-phenylvinylboronic acid and vinyl epoxide, yielding a mixture of linear and branched alcohols. Earlier work showed that SeCSe- and NCN-pincer palladium complexes, but also  $[\text{Pd}_2(\text{dba})_3]$ , are good catalysts for this reaction.<sup>19</sup> Reactivity studies detailed in Szabó's original article showed that the mechanism with SeCSe-pincer palladium catalysts is different from that with  $[\text{Pd}_2(\text{dba})_3]$ , which notably results in different linear-to-branched ratios at full conversion.

Due to the mild conditions of the reaction (room temperature, weak base), decomposition of the ECE-pincer catalyst, thus forming palladium(0), is not likely to occur in the reaction shown

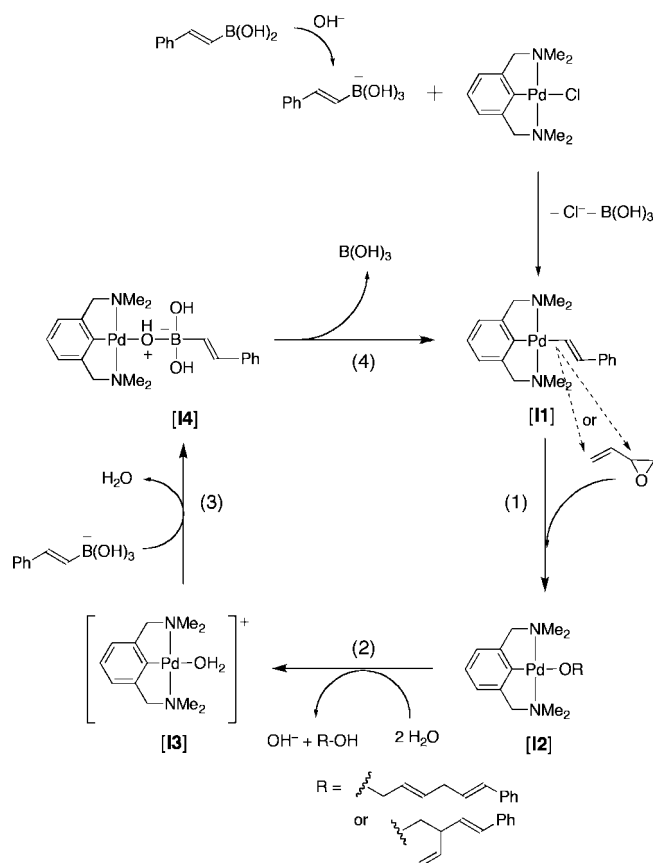
in Scheme 3.<sup>39</sup> When NCN- or SeCSe-pincer palladium catalysts were used, the linear-to-branched ratios observed at full conversion were different from that obtained with [Pd<sub>2</sub>(dba)<sub>3</sub>]. In contrast, it has been shown that under severe reaction conditions (60–110 °C, weak to strong bases) palladium(0) nanoparticles are the real catalytic species when SCS- and PCP-pincer palladium complexes are used as precatalysts in, for example, Heck or Suzuki cross-coupling reactions.<sup>40,41</sup>

Significant differences are observed between NCN-, SeCSe-, and phosphinite PCP-pincer palladium catalysts. Notably, phosphinite PCP-pincer palladium catalysts are inactive in this reaction, which has been attributed to a reduced electron density on palladium when coordinated to the good  $\pi$ -acceptor and poor  $\sigma$ -donor P atoms.<sup>19</sup> In contrast to this lack of reactivity, both NCN-pincer and SeCSe-pincer complexes are efficient catalysts, however, with some marked differences. Experimentally, the NCN-pincer catalysts are less active and less selective (toward the linear isomer) than the SeCSe-pincer catalysts.<sup>19</sup> First, the better  $\sigma$ -donating properties of N (compared to Se) might significantly enhance the rate of the nucleophilic attack of [IS<sub>1</sub>] (Scheme 4) on the epoxide and also decrease the rate of transmetalation. The latter is indeed known to occur faster with electron-poor PCP-pincer palladium catalysts.<sup>15</sup> Second, the steric bulk around the palladium center in each of the pincer-palladium units differs because of the different sizes of the NR<sub>2</sub> versus SeR donor groups.<sup>42</sup>

Our initial assumption, which partly initiated the present study, was that the electronic effects induced by  $\eta^6$ -coordination of a [Ru(C<sub>5</sub>R<sub>5</sub>)<sup>+</sup>] cation (R = H or Me) at the arene ring of NCN-pincer palladium complexes might change the catalytic properties of the resulting complexes.<sup>20,43,44</sup> In the mechanism proposed for SeCSe-pincer catalysts, the nucleophilic attack of the Pd-coordinated phenylvinyl anion on vinyl epoxide is rate determining, and there is a correlation between the nucleophilicity of the transmetalated species and the rate of the reaction. If a similar trend was supposed to exist for NCN-pincer catalysts, electron-poor complexes such as **2**, [3]<sup>+</sup>, or [4]<sup>+</sup> should have a decreased catalytic activity, compared to **1**. In contrast, as observed in Figure 2, all electron-poor complexes are more active than **1**. As a result, the nucleophilic attack of [IS<sub>n</sub>] on the epoxide might not be the rate-determining step of the reaction with such catalysts. This conclusion is confirmed by comparing the catalytic activity of **1**, **8**, and [5]<sup>+</sup>: although the electron-richness of the palladium center in these three complexes is comparable (see Table 2), they appear to have significantly different catalytic activities, with  $t_{50}$  being 2 to 3 times lower for [5]<sup>+</sup> than for **8** or **1**, respectively (see Table 3).

Considering the electron-richness of NCN-pincer palladium centers and the above results, we assume that the nucleophilic attack is fast and the transmetalation much slower with these catalysts, as suggested earlier by Szabó et al.<sup>15</sup> As a consequence, the transmetalation step might become rate determining.

### Scheme 5. Proposed Mechanism for the Cross-Coupling Reaction between *trans*-Phenylvinylboronic Acid and Vinyl Epoxide Catalyzed by NCN-Pincer Palladium Complexes



This hypothesis would explain the surprisingly lower selectivity observed with the more sterically demanding NCN-pincer catalysts, compared to SeCSe-pincer catalysts:<sup>19</sup> if the rate-determining step is transmetalation, attack of the  $\eta^1$ -palladated *trans*-phenylvinyl ligand is fast at both sites of the epoxide, resulting in lower selectivity.

In the last decade, studies have shown that transmetalation is not a single step but a combination of elementary steps.<sup>45–49</sup> In basic media, boronates are recognized as the reactive species for transmetalation of boronic acids to palladium.<sup>50,51</sup> Recently, an intermediate has been experimentally observed, in which the boronate is bound to palladium via an oxygen atom.<sup>46</sup> On the basis of the above consideration and considering the induction period experimentally observed in our catalytic experiments (see Figure 2), we propose the reaction mechanism shown in Scheme 5.

In the first place, slow displacement of the halide by transmetalation takes place to form [II], which allows the pincer complex to enter the catalytic cycle. The first step of the catalytic cycle thus consists of the nucleophilic attack of [II] to vinyl epoxide, which

(39) No palladium black formation was observed in our experiments.

(40) Yu, K. Q.; Sommer, W.; Weck, M.; Jones, C. W. *J. Catal.* **2004**, *226*, 101.

(41) Sommer, W.; Yu, K.; Sears, H. S.; Ji, Y.; Zheng, X.; Davis, R. J.; Sherrill, D.; Jones, C. W.; Weck, M. *Organometallics* **2005**, *24*, 4351.

(42) van Beek, J. A. M.; van Koten, G.; Ramp, M. J.; Coenjaarts, N. C.; Grove, D. M.; Goubitz, K.; Zoutberg, M. C.; Stam, C. H.; Smeets, W. J. J.; Spek, A. L. *Inorg. Chem.* **1991**, *30*, 3059.

(43) Gottker-Schnetmann, I.; White, P. S.; Brookhart, M. *Organometallics* **2004**, *23*, 1766.

(44) van de Kuil, L. A.; Luitjes, H.; Grove, D. M.; Zwikker, J. W.; van der Linden, J. G. M.; Roelofsen, A. M.; Jenneskens, L. W.; Drenth, W.; van Koten, G. *Organometallics* **1994**, *13*, 468.

(45) Braga, A. A. C.; Morgon, N. H.; Ujaque, G.; Lledos, A.; Maseras, F. J. *Organomet. Chem.* **2006**, *691*, 4459.

(46) Sicre, C.; Braga, A. A. C.; Maseras, F.; Cid, M. M. *Tetrahedron* **2008**, *64*, 7437.

(47) Piechaczyk, O.; Cantat, T.; Mezailles, N.; Le Floch, P. *J. Org. Chem.* **2007**, *72*, 4228.

(48) Nova, A.; Ujaque, G.; Maseras, F.; Lledos, A.; Espinet, P. *J. Am. Chem. Soc.* **2006**, *128*, 14571.

(49) Alvarez, R.; Faza, O. N.; de Lera, A. R.; Cardenas, D. J. *Adv. Synth. Catal.* **2007**, *349*, 887.

(50) Braga, A. A. C.; Morgon, N. H.; Ujaque, G.; Maseras, F. J. *Am. Chem. Soc.* **2005**, *127*, 9298.

(51) Goossen, L. J.; Koley, D.; Hermann, H. L.; Thiel, W. *J. Am. Chem. Soc.* **2005**, *127*, 11102.

affords the palladium-alcoholate species [12]. In the presence of an excess of water, quick protonation and ligand exchange yields the free alcohol and the aquo palladium species [13] (step 2). [13] subsequently reacts with a boronate molecule (step 3) to yield the palladium-bound boronate complex [14] proposed by Sicre et al.<sup>46</sup> Step 4 consists of a monomolecular transmetalation, yielding  $B(OH)_3$  and re-forming [11].

Late transition metal–oxygen bonds are known to be kinetically labile.<sup>52</sup> The only known oxygenated ligands bound to NCN-pincer palladium complexes in a monodentate fashion are water and phenolates.<sup>53</sup> For that reason we propose that protonation by water of the bound alcoholate in [12] and exchange of the alcohol for water, i.e., step 2 in Scheme 5, are fast processes. As already discussed above, NCN-pincer palladium species are electron-rich, so that step 1 is also fast. The rate-determining step of the reaction is hence the transmetalation, which is composed of steps 3 and 4.

Considering that the boronate species is an anionic nucleophile, it will be sensitive to the electron density on palladium. Removing electron density from the palladium center, either by *para*-NO<sub>2</sub> substitution or by  $\eta^6$ -coordination of  $[Ru(C_5R_5)]^+$ , would increase the rate of step 3, hence the rate of the reaction. This is what was experimentally observed: electron-poor NCN-pincer palladium catalysts **2** and **[3]<sup>+</sup>** and **[4]<sup>+</sup>** are more active than **1**. The mere additional positive charge brought about by the cationic ruthenium fragment will facilitate ion pair formation with the anionic boronate species, which would explain why cationic catalysts **[3]<sup>+</sup>**–**[5]<sup>+</sup>** are overall more active than **1**. In step 4 steric congestion might also play an important role. On the basis of the work of Sicre et al.,<sup>46</sup> it is likely that the transition state of this monomolecular elementary step involves a hindered five-coordinate species with an  $\eta^2$ -coordinated phenylvinyl ligand, which ultimately evolves into  $\eta^1$ -binding of the phenylvinyl organic group in [11]. Our catalytic results suggest that releasing steric congestion around the palladium center increases the catalytic activity of the NCN-pincer catalysts: both **[3]<sup>+</sup>** and **[5]<sup>+</sup>** are more active than complex **[4]<sup>+</sup>**. In the former the Cp ligand is less hindering than Cp\*; in the latter the  $[Ru(C_5Me_5)]^+$  fragment is much farther from palladium (cf. the Pd–Ru distance in Table 1). A less hindered catalyst might lead to step 4 being faster, hence to a faster reaction rate.

Overall, complex **[5]<sup>+</sup>** shows a surprisingly high catalytic activity, which might arise from (1) the presence of an additional positive charge on the catalyst and (2) a reduced steric congestion. In addition, both faces of the catalyst are available for the approach of the nucleophile with **[5]<sup>+</sup>**, whereas with **[3]<sup>+</sup>** and **[4]<sup>+</sup>** one face is sterically hindered due to the  $\eta^6$ -coordinated  $[Ru(C_5R_5)]^+$  fragment. This example highlights the limited impact of intramolecular electronic effects in our catalytic results; thus, “through-bond” interactions are not affecting too much the catalytic activity of NCN-pincer palladium catalysts. On the contrary, steric hindrance and geometry seem to play a major role here, as well as more unusual effects related to the presence of a positive charge that modify ion pair formation (“through-space” interactions).

It might be noted that the evolution of the linear-to-branched ratio with reaction progress showed that selectivity changed

(from 0 to 2.3) during the course of the reaction, with the branched product being formed faster than the linear one (see Figure 3). At high conversions, the linear-to-branched ratio converged toward the same value of about 2.3, independent of the nature of the NCN-pincer palladium catalyst. The occurrence of a process involving interconversion between the linear and branched alcohols seems unlikely, as it would imply reversible C–C bond cleavage/bond formation. The present results suggest, however, that the disappearance of the epoxide and/or the formation of the products might influence the selectivity of the reaction. Alcohols are known to bind reversibly to boronic acids.<sup>54,55</sup> Lewis bases such as epoxides might reversibly bind to boronic acids, but also to the palladium center.<sup>56</sup> Several equilibria between vinyl epoxide, the linear and branched alcohols, and the Lewis acids present in solution might be considered, which would play a role in the rate of formation of the linear and/or branched products when the concentrations of the epoxide and alcohols vary. Additional mechanistic studies must be undertaken to provide a better picture of the mechanism shown in Scheme 5.

## Conclusion

In this report, we present a series of ruthenium–palladium  $\eta^6, \eta^1$ -bimetallic complexes of the NCN-pincer type, in which the organic ligand is at the same time  $\eta^6$ - and  $\eta^1$ -coordinated to two different metal centers. Comparison of the X-ray crystal structures of **[4](BF<sub>4</sub>)**,<sup>26</sup> **[5](BF<sub>4</sub>)**, and **[9](BF<sub>4</sub>)**<sup>31</sup> shows that steric hindrance between the N-methyl groups of the NCN-pincer ligand and the bulky Cp\* ligand increases in the series **[9](BF<sub>4</sub>)** < **[5](BF<sub>4</sub>)** < **[4](BF<sub>4</sub>)**. We tested the catalytic activity of the ruthenium-modified NCN-pincer palladium complexes **[3]<sup>+</sup>**–**[5]<sup>+</sup>** in the cross-coupling reaction between *trans*-phenylvinylboronic acid and vinyl epoxide: they have a better catalytic activity than their monometallic palladium precursor **1**. DFT calculations performed on the transmetalated species **[IS<sub>n</sub>]** and palladium oxidation potentials measured in solution agree with an opposite reactivity trend compared to previously studied SeCSe-pincer palladium catalysts: electron-poor NCN-pincer palladium complexes have a higher catalytic activity than electron-rich ones. On the basis of this observation we propose a reaction mechanism where transmetalation is rate determining (Scheme 5). According to our analysis, the positive charge induced by the  $\eta^6$ -coordinated ruthenium fragment facilitates the nucleophilic attack of *trans*-phenylvinylboronate on palladium (step 3). Meanwhile, the diminished steric congestion in **[5]<sup>+</sup>** explains (step 4) its surprisingly better catalytic properties. Finally, kinetic studies have brought intriguing information on the evolution of the linear/branched ratio during the course of the reaction, which could not be observed by looking only at the final state of the catalytic system.

## Experimental Part

**Synthesis.** All reactions using sensitive reagents were performed under an atmosphere of dinitrogen using Schlenk techniques. THF and Et<sub>2</sub>O were dried over Na/benzophenone. MeCN and CH<sub>2</sub>Cl<sub>2</sub> were dried over CaH<sub>2</sub>, and all solvents were freshly distilled under nitrogen prior to use. <sup>1</sup>H (300.1/400.0 MHz) and <sup>13</sup>C (75.5/100.6 MHz) NMR spectra were recorded on a Varian INOVA 300 or

(52) Bryndza, H. E.; Fong, L. K.; Paciello, R. A.; Tam, W.; Bercaw, J. E. *J. Am. Chem. Soc.* **1987**, *109*, 1444.

(53) Alsters, P. L.; Baesjou, P. J.; Janssen, M. D.; Kooijman, H.; Sichererroetman, A.; Spek, A. L.; van Koten, G. *Organometallics* **1992**, *11*, 4124.

(54) Fujita, N.; Shinkai, S.; James, T. D. *Chem.–Asian J.* **2008**, *3*, 1076.

(55) Selander, N.; Kipke, A.; Sebelius, S.; Szabo, K. J. *J. Am. Chem. Soc.* **2007**, *129*, 13723.

(56) Solin, N.; Kjellgren, J.; Szabo, K. J. *J. Am. Chem. Soc.* **2004**, *126*, 7026.

400 MHz spectrometer;  $^{31}\text{P}\{^1\text{H}\}$  (121.5 MHz) and  $^{19}\text{F}$  (376 MHz) NMR spectra were recorded on a Varian INOVA 400 MHz spectrometer. Chemical shift values are reported in ppm ( $\delta$ ) relative to  $\text{Me}_4\text{Si}$  ( $^1\text{H}$  and  $^{13}\text{C}$  NMR). MALDI-TOF measurements were carried out on an Applied Biosystems Voyager DE-STR MALDI-TOF MS. Elemental analyses were performed by H. Kolbe Microanalysis Laboratories, Mülheim, Germany. GC analyses were performed on a Perkin-Elmer Clarus-500 gas chromatograph. GC-MS measurements were measured on a Perkin-Elmer AutosystemXL gas chromatograph with an attached Perkin-Elmer Turbo-mass Upgrade mass spectrometer. For column chromatography, Merck silica gel 60 (230–400 mesh) was used. All standard reagents were purchased from Acros Organics or Sigma-Aldrich, and used as received. *para*-Phenyl NCN-pincer ligand **7**,<sup>57</sup> pincer metal complexes **1**<sup>58</sup> and **2**,<sup>13</sup> and ruthenated derivatives **[9]**<sup>+</sup>,<sup>29</sup> **[3]**<sup>+</sup>, and **[4]**<sup>+</sup><sup>26</sup> were prepared according to literature procedures.

**8**: A 1.69 g amount of ligand **7** (5.78 mmol) was weighed in a flame-dried Schlenk flask and put under a nitrogen atmosphere. Then 40 mL of dry pentane was added, and the solution was cooled to  $-78$  °C. A 3.5 mL amount of *n*-BuLi (as 1.6 M solution in hexanes, 5.6 mmol) was added dropwise to give an orange solution, which was stirred at  $-78$  °C for 30 min. The cooling bath was then removed, and the solution warmed to room temperature overnight (18 h) to yield a yellowish suspension. Pentane was evaporated, replaced by 100 mL of dry diethyl ether, the suspension was cooled to  $-78$  °C, and 1.96 g of  $\text{PdCl}_2(\text{SEt}_2)_2$  (5.49 mmol) was slowly added under a flow of dinitrogen. The suspension was stirred 1 h at  $-78$  °C, then allowed to warm to room temperature overnight (24 h) under nitrogen. Diethyl ether was evaporated, and the crude material was dissolved in 200 mL of dichloromethane, washed with water and brine, dried over  $\text{MgSO}_4$ , and filtered over Celite. Addition of 100 mL of hexane and slow evaporation of  $\text{CH}_2\text{Cl}_2$  afforded 1.48 g of crystalline product (62%). Characterization was identical to the published data.<sup>20</sup>

**[5]**<sup>+</sup>: A 159 mg amount of **8** (388  $\mu\text{mol}$ ) was weighed in a dry Schlenk flask and put under inert atmosphere. A solution of  $[\text{RuCp}^*(\text{MeCN})_3](\text{BF}_4)^{59}$  (174 mg, 389  $\mu\text{mol}$ ) in 5 mL of dry dichloromethane was added, and the mixture stirred under nitrogen at room temperature for 3 days. The crude solution was put on top of an 80 mL silica gel column and eluted with  $\text{CH}_2\text{Cl}_2$  containing 1–3% methanol to remove unreacted starting materials. Yield: 229 mg of **[5](BF<sub>4</sub>)** as a whitish powder (81%).  $^1\text{H}$  NMR  $\delta$  (400 MHz, ppm in acetone-*d*<sub>6</sub>): 7.31 (s, 2H, m), 6.54 (d, 2H, o', *J* 5.9), 6.16 (t, 2H, m', *J* 6.2), 6.11 (t, 1H, p', *J* 5.7), 4.20 (s, 4H,  $\text{CH}_2\text{N}$ ), 2.92 (s, 12H,  $\text{NMe}_2$ ), 1.89 (s, 15H,  $\text{C}_5\text{Me}_5$ ).  $^{13}\text{C}$  NMR  $\delta$  (100 MHz, ppm in acetone-*d*<sub>6</sub>): 162.2 (i), 147.6 (o), 129.5 (p), 119.3 (m), 103.5 (i'), 97.1 ( $\text{C}^{\text{IV}}\text{R}_3$ ), 88.4, 88.2, 85.4 (o', m', p'), 75.3 ( $\text{CH}_2\text{N}$ ), 53.2 ( $\text{NMe}_2$ ), 10.3 ( $\text{C}_5\text{Me}_5$ ).  $^{19}\text{F}$  NMR  $\delta$  (376 MHz, ppm in acetone-*d*<sub>6</sub>):  $-152.1$  (s). MALDI-TOF *m/z* (calc): 645.11 (645.08,  $[\text{M} - \text{BF}_4]^+$ ). C, H, N: 45.92/5.23/3.83 (calc); 45.79/5.20/3.78 (found).

**X-ray Crystallography.** All reflection intensities were measured using a Nonius KappaCCD diffractometer (rotating anode) with graphite-monochromated  $\text{Mo K}\alpha$  radiation ( $\lambda = 0.71073$  Å) using the program COLLECT.<sup>60</sup> The program PEAKREF<sup>61</sup> was used to refine the cell dimensions. Data reduction was done using the program EVALCCD.<sup>62</sup> The structure was solved with the program

DIREDF99<sup>63</sup> and was refined on  $F^2$  with SHELXL-97.<sup>64</sup> The temperature of the data collection was controlled using the Oxford Cryostream 600 system (manufactured by Oxford Cryosystems). The H-atoms were placed at calculated positions (AFIX 23, AFIX 43, or AFIX 137) with isotropic displacement parameters having values 1.2 or 1.5 times  $U_{\text{eq}}$  of the attached C-atom. Illustrations and structure validations were done with PLATON.<sup>65</sup>

**Crystal Growth.** A dichloromethane solution of the complex (5 mg/mL) was put in an open 2 mL vial, which was contained in a closed 20 mL vial. The larger vial contained about 6 mL of hexane. As vapor diffusion took place, crystal growth occurred at room temperature without any additional effort, and crystals appeared at the bottom of the smaller vial after one to two weeks. X-ray structure data for **[5]**<sup>+</sup>:  $\text{C}_{28}\text{H}_{38}\text{ClN}_2\text{PdRu} \cdot \text{BF}_4$ ,  $M_r = 732.33$ , colorless plate,  $0.46 \times 0.18 \times 0.06$  mm<sup>3</sup>, triclinic,  $P\bar{1}$  (no. 2),  $a = 14.1334(5)$  Å,  $b = 14.7569(5)$  Å,  $c = 16.1141(6)$  Å,  $\alpha = 78.019(2)^\circ$ ,  $\beta = 77.718(2)^\circ$ ,  $\gamma = 63.285(2)^\circ$ ,  $V = 2909.14(18)$  Å<sup>3</sup>,  $Z = 4$ ,  $D_x = 1.672$  g cm<sup>-3</sup>,  $\mu = 1.27$  mm<sup>-1</sup>; 41 951 reflections were measured at 150(2) K after the crystal had been flash-cooled from room temperature. Multiscan empirical absorption corrections were applied to the data using the program TWINABS.<sup>66</sup>  $T_{\text{min}} = 0.710$  and  $T_{\text{max}} = 0.930$ ; 12 040 reflections were unique ( $R_{\text{int}} = 0.0583$ ), of which 9157 were observed with the criterion of  $I > 2\sigma(I)$ ; 784 parameters were refined with 236 least-squares restraints.  $R_1/wR_2 [I > 2\sigma(I)]$ : 0.060/0.110.  $R_1/wR_2$  [all reffs]: 0.096/0.128.  $S = 1.15$ . The residual electron density was found between  $-1.25$  and  $1.49$  e Å<sup>-3</sup>. Crystals were nonmerohedrally twinned with a 2-fold axis along the  $[-1\ 1\ 0]$  direction as the twin operation. The minor twin fraction refined to 0.467(1). Occupancy factors for the major components of the disordered counteranions were 0.65(3) and 0.57(1).

**Catalytic Studies.** Eight experiments were run simultaneously using a ChemSpeed automated apparatus. In each reaction vessel, 1.04 g (3.2 mmol) of  $\text{Cs}_2\text{CO}_3$ , 1.5 mL of a 1.06 M solution of *trans*-phenylvinylboronic acid in tetrahydrofuran (1.6 mmol), 400  $\mu\text{L}$  of water, 100  $\mu\text{L}$  of dihexyl ether (internal reference), and 160  $\mu\text{L}$  (1.2 equiv) of vinyl epoxide were added one after another. Subsequently, 1 or 0.25 mol % palladium catalyst was added as a solid, and the vial containing the catalyst was rinsed with 1.5 mL of tetrahydrofuran that was added to the vessel. After preparation of the 8 vessels, the vessel holder was mounted on the ChemSpeed system thermostated at 25 °C, and  $t = 0$  was set upon starting stirring at 1000 rpm. At regular intervals, stirring was stopped, the biphasic mixture left untouched during 10 s, and 50  $\mu\text{L}$  of the upper layer (THF) taken via a syringe in each of the 8 vessels and poured into 3.0 mL of dichloromethane. Stirring of the vessels was then switched on before workup of the 8 samples was started. Workup consisted in adding 1.0 mL of 1 M NaOH to the dichloromethane phase and extracting it three times to remove unreacted boronic acid from the organic layer. The dichloromethane phase was analyzed by GC using dihexyl ether as internal reference.

**DFT Calculation.** All DFT calculations were performed using B3LYP/LANL2DZ as implemented in the GAMESS-UK program<sup>35</sup> and using MOLDEN<sup>67</sup> to visualize the structures and edit Z-matrices. The geometry found in the X-ray structures of complexes **[4]**<sup>+</sup> and **[5]**<sup>+</sup> was used as a starting point, using for **[5]**<sup>+</sup> the geometry containing Pd1 and Ru1. The chloride ligand was replaced

(57) Steenwinkel, P.; James, S. L.; Grove, D. M.; Veldman, N.; Spek, A. L.; van Koten, G. *Chem.-Eur. J.* **1996**, *2*, 1440.

(58) Terheijden, J.; van Koten, G.; Mul, W. P.; Stufkens, D. J.; Muller, F.; Stam, C. H. *Organometallics* **1986**, *5*, 519.

(59) Fagan, P. J.; Ward, M. D.; Calabrese, J. C. *J. Am. Chem. Soc.* **1989**, *111*, 1698.

(60) Nonius. COLLECT; Nonius B. V.: Delft, The Netherlands 1998.

(61) Schreurs, A. M. M. PEAKREF; Utrecht University: Utrecht, The Netherlands, 2005.

(62) Duisenberg, A. J. M.; Kroon-Batenburg, L. M. J.; Schreurs, A. M. M. *J. Appl. Crystallogr.* **2003**, *36*, 220.

(63) Beurskens, P. T.; Admiraal, G.; Beurskens, G.; Bosman, W. P.; Garcia-Granda, S.; Gould, R. O.; Smits, J. M. M.; Smykalla, C. The DIREDF99 Program System; Technical Report of the Crystallography Laboratory, University of Nijmegen; University of Nijmegen: Nijmegen, The Netherlands, 1999.

(64) Sheldrick, G. M. SHELXL97; University of Göttingen: Göttingen, Germany, 1997.

(65) Spek, A. L. *J. Appl. Crystallogr.* **2003**, *36*, 7.

(66) Sheldrick, G. M. TWINABS; University of Göttingen: Göttingen, Germany, 2003.

(67) Schaftenaar, G.; Noordik, J. H. *J. Comput.-Aided Mol. Des.* **2000**, *14*, 123.

by a *trans*-phenylvinyl ligand parallel to the arene ring, and the structures were minimized without symmetry constraint (convergence threshold:  $10^{-4}$ ). A chloride counteranion was then added on the side of the ruthenium-arene complex, and the geometries were minimized again, to give the neutral geometries shown in Figure 4.

**Acknowledgment.** We gratefully acknowledge the support of this research by Utrecht University. This work was supported in part (M.S., A.L.S.) by the Council for the Chemical Sciences of The Netherlands Organization for

Scientific Research (CW-NWO) and in part by the Stichting Nationale Computerfaciliteiten (National Computing Facilities Foundation, NCF) for the use of supercomputer facilities.

**Supporting Information Available:** Crystallographic data for [5](BF<sub>4</sub>) in CIF format, as well as the Cartesian coordinates for the DFT-minimized structures shown in Scheme 4, are available free of charge via the Internet at <http://pubs.acs.org>.

OM801200C